



TITLE:

# Structure and formation mechanism of Ge E ' center from divalent defects in Ge-doped SiO<sub>2</sub> glass

AUTHOR(S):

Uchino, T; Takahashi, M; Yoko, T

---

CITATION:

Uchino, T ...[et al]. Structure and formation mechanism of Ge E ' center from divalent defects in Ge-doped SiO<sub>2</sub> glass. PHYSICAL REVIEW LETTERS 2000, 84(7): 1475-1478

ISSUE DATE:

2000-02-14

URL:

<http://hdl.handle.net/2433/50390>

RIGHT:

Copyright 2000 American Physical Society

## Structure and Formation Mechanism of Ge $E'$ Center from Divalent Defects in Ge-doped SiO<sub>2</sub> Glass

Takashi Uchino,\* Masahide Takahashi, and Toshinobu Yoko

*Institute for Chemical Research, Kyoto University, Uji, Kyoto 611-0011, Japan*

(Received 16 July 1999)

We have performed *ab initio* quantum-chemical calculations on clusters of atoms modeling a divalent Ge defect in Ge-doped SiO<sub>2</sub> glasses. It has been found that the divalent Ge defect interacts with a nearby GeO<sub>4</sub> tetrahedron, forming complex structural units that are responsible for the observed photoabsorption band at  $\sim 5$  eV. We have shown that these structural units can be transformed into two equivalent Ge  $E'$  centers by way of the positively charged defect center.

PACS numbers: 61.43.Fs, 61.46.+w, 61.72.Ji

Photosensitivity and photoinduced holographic Bragg gratings were discovered in Ge-doped SiO<sub>2</sub> glasses about 20 years ago [1]. Presently photoinduced Bragg fiber and planar waveguide gratings in the glasses are widely used in telecommunication technology for wavelength-divided multiplexing, signal shaping, fiber lasers, and amplifiers, etc. In contrast to these spectacular advances in practical applications, however, the fundamental understanding of the respective photoinduced processes in glass is incomplete. In Ge-doped SiO<sub>2</sub> glasses, there exists an intense photoabsorption band at 5 eV [2], which is believed to be related to oxygen deficiency. Although the defect center associated with the 5-eV band most likely plays an important role in the photorefractive index change induced by ultraviolet (uv) irradiation [3], the details of the processes and mechanisms involved have remained obscure.

It has been demonstrated that the 5-eV band is composed at least of two components centered at 5.06 and 5.16 eV [4]. The 5.06-eV band is bleached upon uv irradiation to generate the paramagnetic oxygen vacancy, called the Ge  $E'$  center [4]. The 5.06-eV band was once ascribed to the unrelaxed neutral oxygen vacancy [4], but the physical origin of this band is still under discussion [5,6]. On the other hand, the 5.16-eV band, which is pumping the photoluminescence emissions at 3.2 and 4.3 eV, was attributed to divalent Ge defects having a lone pair of electrons, namely,  $\text{—}\ddot{\text{Ge}}\text{—}$  [4,7]. This assignment was recently supported by first-principle quantum-chemical calculations on clusters of atoms modeling a divalent Ge defect in Ge-doped SiO<sub>2</sub> glasses [8,9]. While the 5.16-eV band is almost stable against low-power uv exposure [4], irradiation with a dense flux of uv photons such as KrF excimer laser pulses can induce the appreciable photobleaching for this band [10–12], which accompanies the generation of Ge  $E'$  (and other unknown defect centers) as in the case of the bleaching of the 5.06-eV band [11]. This result suggests that the defect centers associated with the 5.16-eV band can be a precursor of Ge  $E'$  centers depending on the power densities of uv photons. However, it is not easy to understand why the bleaching of the 5.16-eV band results in the formation of Ge  $E'$  if this band is due to the divalent Ge defects [6].

Although several models have been proposed to explain this problem [6,11–14], no satisfactory explanation has yet been given.

In this paper we, therefore, investigate the formation mechanism of Ge  $E'$  centers from the divalent Ge defect in Ge-doped SiO<sub>2</sub> glasses by using *ab initio* cluster model calculations at the Hartree-Fock (HF) level. It has been demonstrated that *ab initio* quantum-chemical cluster approaches are useful to investigate the structure and vibrational properties of glassy systems [15,16]. In particular, since the defect states in glasses are in general quite localized, their structure and energy states will be reasonably modeled by the cluster calculations [5,8,9,17]. Appropriate cluster models hence allow us to investigate the geometries and electronic structures of the defect centers in glasses, and the calculated results will shed new light on the unsolved problem concerning the formation mechanism of Ge  $E'$  centers associated with the photobleaching of the 5.16-eV band and other photoinduced phenomena of interest in Ge-doped SiO<sub>2</sub> glasses.

The photoabsorption (PA) and photoluminescence (PL) properties of the divalent defects have been previously studied by means of *ab initio* quantum-chemical calculations on the (H<sub>3</sub>TO)<sub>2</sub>T cluster (where T is Ge or Si) [8,9], and the calculated PA and PL energies for the clusters have been shown to agree well with the corresponding experimental values. In this work, we, therefore, used a similar cluster, [(OH)<sub>3</sub>SiO]<sub>2</sub>Ge, as a model for the divalent Ge defect though the dangling bonds of the model cluster were not saturated by H atoms but by OH groups. Furthermore, we added a (OH)<sub>3</sub>Ge—O—Ge(OH)<sub>3</sub> cluster to the above [(OH)<sub>3</sub>SiO]<sub>2</sub>Ge cluster to consider a possible effect of the condensed environments in which the divalent Ge defect actually resides. In actual Ge-doped silica, a divalent Ge defect is most certainly surrounded by one or more TO<sub>4</sub> units in addition to the two TO<sub>4</sub> units that are originally bonded to the center  $\text{—}\ddot{\text{Ge}}\text{—}$  atom. It is natural to expect that these nearby TO<sub>4</sub> units play a key role in generating, if possible, Ge  $E'$  centers upon uv irradiation. The geometry of the ground-state singlet ( $S_0$ ) structure of the cluster was fully optimized at the HF level of theory with the

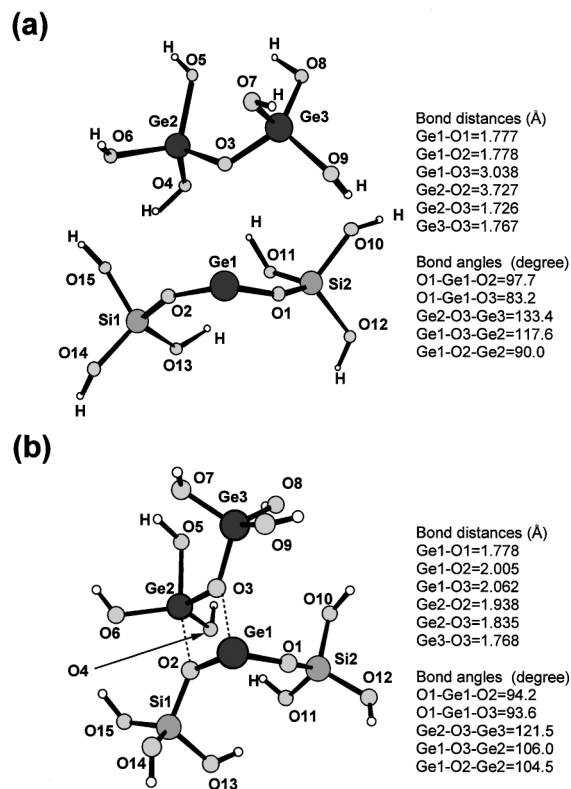


FIG. 1. Two equilibrium geometries of a ground-state singlet for a  $\text{Ge}_3\text{Si}_2\text{O}_{15}\text{H}_{12}$  cluster optimized at the HF/6-311G(d) level: (a) lower (model 1a) and (b) higher (model 1b) energy configurations. Principal bond distances and bond angles are also shown.

polarized 6-311G(d) basis set [18] by using analytical gradient methods. All *ab initio* molecular orbital calculations were carried out using the GAUSSIAN 94 computer program [19] on a supercomputer CRAY T94/4128.

As a result of the geometry optimizations, we found that there exist at least two minimum energy configurations for  $S_0$  (see Fig. 1), which are separated only by 0.19 eV in total energy. Table I shows the calculated bond overlap populations,  $n$ , and atomic charges,  $Q$ ,

obtained from a Mulliken population analysis. The lower energy configuration [model 1a; see Fig. 1(a)] can be regarded as a simple combination of the  $[(\text{OH})_3\text{SiO}_2]\text{Ge}$  and  $(\text{OH})_3\text{Ge}-\text{O}-\text{Ge}(\text{OH})_3$  clusters. The association energy,  $\Delta E$ , obtained by a difference between the total energies of model 1a and its constituent optimized clusters was calculated to be 0.61 eV. On the other hand, the higher energy configuration shown in Fig. 1(b) (model 1b,  $\Delta E = 0.42$  eV) results from the considerable structural reorganization between the two initial  $[(\text{OH})_3\text{SiO}_2]\text{Ge}$  and  $(\text{OH})_3\text{Ge}-\text{O}-\text{Ge}(\text{OH})_3$  clusters. That is, in model 1b, O2 and O3 tend to form additional covalent bonds with Ge2 and Ge1, respectively, forming an edge-sharing unit composed of a three-coordinated Ge (Ge1) and a five-coordinated Ge (Ge2). It should be noted, however, that the configuration of model 1b might require a substantial distortion in forming such an edge-sharing structure, which probably explains the higher total energy as compared with that of model 1a. Furthermore, in actual glassy systems the formation of model 1b will be accomplished at the expense of the topology of the surrounding glass network, causing additional strain energies on the medium-range ( $\sim 5$ – $\sim 10$  Å) length scale. Thus, we consider that model 1a will be more realistic as a model of the divalent Ge in actual Ge-doped  $\text{SiO}_2$  glass.

In order to obtain excitation energies for the models 1a and 1b, we employed time-dependent density-functional response theory (TD DFRT) [20]. It has been demonstrated that the average absolute error of the TD DFRT is closer to that of the more costly correlated *ab initio* methods such as the configuration interaction method [20]. The TD DFRT excitation energies were calculated for the HF/6-311G(d) geometries at the Becke's 1993 hybrid exchange functional with the Lee-Yang-Parr correlation energy functional [21] (B3LYP) level with the 6-311G(d) basis set augmented by two sets of diffuse *s* and *p* functions on Ge1. The  $S_0$ - $S_1$  transitions of models 1a and 1b were calculated to be 5.29 and 5.49 eV, respectively, which are both in reasonable agreement with the observed transition at 5.16 eV. This

TABLE I. Mulliken bond overlap populations,  $n$ , and atomic charge,  $Q$ , for models 1–3 calculated at the HF/6-311G(d) level. Values in parentheses show the atomic spin densities.

	Model 1a	Model 1b	Model 2	Model 3
$n(\text{Ge1}-\text{O1})$	0.194	0.256	0.486	0.341
$n(\text{Ge1}-\text{O2})$	0.213	0.043	0.366	0.387
$n(\text{Ge1}-\text{O3})$	0.015	−0.036	0.064	0.370
$n(\text{Ge2}-\text{O2})$	0.020	0.243	0.016	0.016
$n(\text{Ge2}-\text{O3})$	0.477	0.244	0.157	0.008
$n(\text{Ge2}-\text{O4})$	0.518	0.509	0.622	0.388
$n(\text{Ge2}-\text{O5})$	0.499	0.457	0.526	0.435
$n(\text{Ge2}-\text{O6})$	0.518	0.524	0.554	0.397
$Q(\text{Ge1})$	1.259	1.292	1.803(0.898)	1.719(0.897)
$Q(\text{Ge2})$	2.071	2.119	2.166(0.002)	1.564(0.882)
$Q(\text{Ge3})$	2.059	2.134	2.157(−0.003)	2.078(0.003)
$Q(\text{O1})$	−1.052	−1.064	−1.009(0.030)	−1.040(0.020)
$Q(\text{O2})$	−1.062	−1.185	−1.088(0.040)	−1.051(0.039)
$Q(\text{O3})$	−1.149	−1.268	−1.341(0.018)	−1.126(0.031)

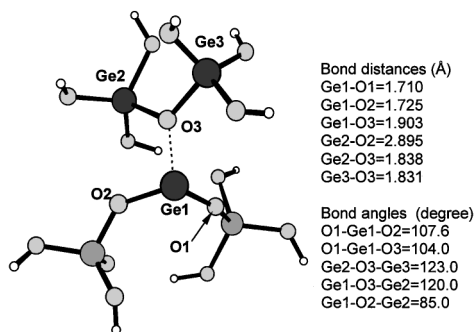


FIG. 2. A positively charged  $(\text{Ge}_3\text{Si}_2\text{O}_{15}\text{H}_{12})^+$  cluster model (model 2) fully optimized at the HF/6-311G(d) level. For geometry optimization, we used the structure of both models 1a and 1b as initial geometries.

result indicates that although model 1a is still a promising model of the Ge divalent defect in Ge-doped  $\text{SiO}_2$  glass, model 1b cannot completely be ruled out as a model of the defect center that is responsible for the PA band at  $\sim 5$  eV.

The electronic transitions accompanying the PA and PL bands correspond to the irradiation processes induced by low-power density irradiation and do not cause any structural change (or photobleaching) in the glass structure [4,11]. On the other hand, the high-power density irradiation such as an excimer laser results in the photobleaching of the 5.16-eV band [10–12] as mentioned before. Because of the high-power density of the laser pulses, electrons in the valence orbital will be excited to the conduction band via two photon processes [11], and, accordingly, a positively charged defect center is expected to be formed. It is hence interesting to reoptimize the geometry of model 1a as well as model 1b by assuming a total charge of +1 for the cluster. We did not impose any structural constraint in optimizing the geometry of this positively charged cluster, which will be referred to as model 2.

It is worth mentioning that both models 1a and 1b converged on the same positively charged cluster shown in Fig. 2. The Ge1—O1 (1.710 Å) and Ge1—O2 (1.725 Å) bond distances in model 2 are considerably shorter than the corresponding bond distances in models 1a and 1b, and there exists no substantial interaction between O2 and Ge2 in model 2. It should also be noted that the Ge1—O3 bond distance in model 2 (1.903 Å) is shorter than that in models 1a (3.038 Å) and 1b (2.062 Å), indicating that the interaction between Ge1 and O3 becomes stronger as a result of the ionization process. The atomic spin density on Ge1 in model 2 is  $\sim 0.9$ , and its atomic charge is larger than that in models 1a and 1b by  $\sim 0.5$  (see Table I). Thus, the

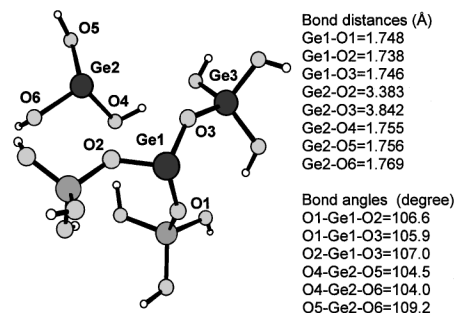
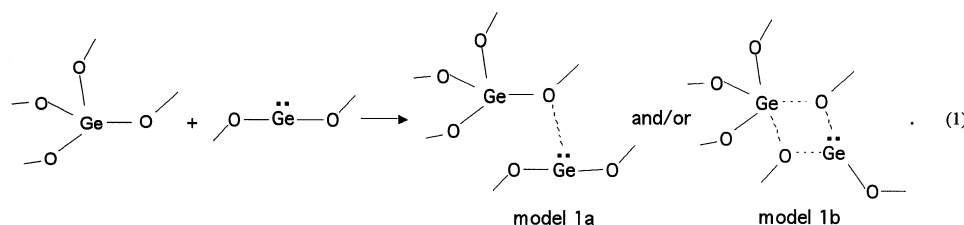


FIG. 3. A  $\text{Ge}_3\text{Si}_2\text{O}_{15}\text{H}_{12}$  cluster model of a triplet state (model 3) fully optimized at the restricted open HF/6-311G(d) level. For geometry optimization, we used the structure of model 2 as an initial geometry.

center Ge1 atom in model 2 can be regarded as a positively charged defect center, and the shorter Ge1—O3 bond mentioned above can be interpreted in terms of the stronger Coulomb interaction between Ge1 and O3 as compared with that in models 1a and 1b. It has also been found that the lowest unoccupied molecular orbital spread evenly over the empty nonbonding orbitals on the oxygen atoms in the  $\text{GeO}_4$  units in model 2. We, therefore, suggest that the electron excited to the conduction band will be trapped at a nearby  $\text{GeO}_4$  unit, forming a Ge electron center [11,14,22].

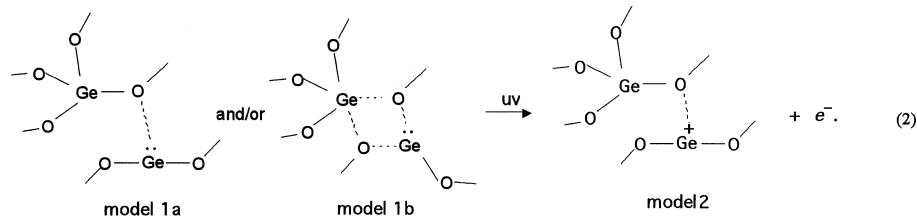
What happens when this positively charged cluster is neutralized? In order to simulate such a process, we then optimized the geometry of model 2 by assuming a triplet state at the restricted open HF level. Such a triplet defect was indeed found in  $x$ - or  $\gamma$ -irradiated fused silica [23–25], and the triplet center is observed only for glasses having 5.0-eV band prior to irradiation [24], in agreement with the present model. The optimized geometry of the triplet state, which we call model 3, is illustrated in Fig. 3. It is quite interesting to note that the resultant geometry of model 3 is completely different from that of the previous clusters. We see from Fig. 3 that the distance between Ge2 and O3 tends to become wide apart, resulting in two almost equivalent  $\text{GeO}_3$  units. The atomic spin densities for Ge1 and Ge2 in model 3 are calculated to be 0.897 and 0.882, respectively, indicating that these two  $\text{GeO}_3$  units are unambiguously Ge  $E'$  centers.

On the basis of the above calculated results, we can propose a possible mechanism of the formation of Ge  $E'$  centers from a divalent Ge defect as follows. First, the divalent Ge defect interacts with the adjacent  $\text{GeO}_4$  unit, and the following structural units are expected to be formed (see models 1a and 1b):

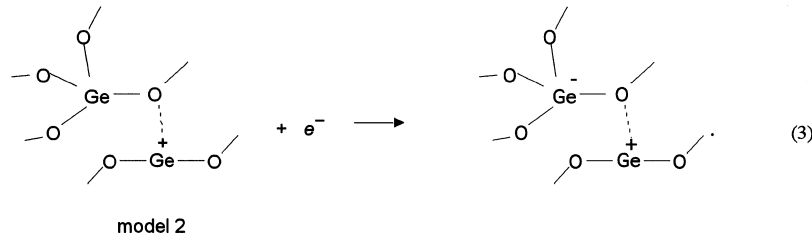


Second, irradiation of the high-power laser excites one of the lone pair electrons on the divalent Ge defect to the

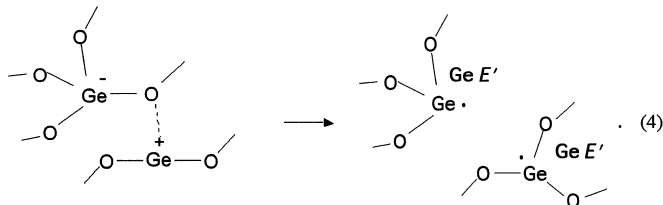
conduction band, forming a positively charged Ge center (see model 2):



Third, the electron in the conduction band is trapped by the  $\text{GeO}_4$  unit adjacent to the divalent Ge defect:



Finally, the electron-hole recombination occurs, and the two equivalent Ge  $E'$  centers are eventually generated (see model 3):



In conclusion, the present calculations have shown that the divalent Ge defect and its adjacent  $\text{GeO}_4$  unit interact with each other, forming the combined structural units shown in Fig. 1(a) and/or Fig. 1(b). We have further demonstrated that these structural units can be transformed into two equivalent  $\text{GeO}_3$  units having an unpaired electron, namely, Ge  $E'$  centers, via positively charged defect centers. We consider that the structural conversion mechanism proposed in this study plays a vital role in the refractive index changes of Ge-doped  $\text{SiO}_2$  glasses induced by high-power uv irradiation.

We would like to thank the Supercomputer Laboratory, Institute for Chemical Research, Kyoto University, for providing the computer time to use the CRAY T-94/4128 supercomputer.

\*Email address: uchino@scl.kyoto-u.ac.jp

- [1] K.O. Hill, Y. Fujii, D.C. Johnson, and B.S. Kawasaki, Appl. Phys. Lett. **32**, 647 (1978).
- [2] A.J. Cohen and H.L. Smith, J. Phys. Chem. Solids **7**, 301 (1958).
- [3] V. Mizrahi and R.M. Atkins, Electron. Lett. **28**, 2210 (1992).
- [4] H. Hosono *et al.*, Phys. Rev. B **46**, 11 445 (1992).

- [5] B. B. Stefanov and K. Raghavachari, Phys. Rev. B **56**, 5035 (1997).
- [6] L. Skuja, J. Non-Cryst. Solids **239**, 16 (1998).
- [7] L. N. Skuja, A. N. Streletsky, and A. B. Pakovich, Solid State Commun. **50**, 1069 (1984); L. Skuja, J. Non-Cryst. Solids **149**, 77 (1992).
- [8] B. L. Zhang and K. Raghavachari, Phys. Rev. B **55**, R15 993 (1997).
- [9] G. Pacchioni and R. Ferrario, Phys. Rev. B **58**, 6090 (1998).
- [10] R. M. Atkins, V. Mizrahi, and T. Erdogan, Electron. Lett. **29**, 385 (1993).
- [11] J. Nishii *et al.*, Phys. Rev. B **52**, 1661 (1995).
- [12] M. Gallagher and U. Osterberg, J. Appl. Phys. **74**, 2771 (1993).
- [13] M. Essid *et al.*, J. Non-Cryst. Solids **246**, 39 (1999).
- [14] M. Fujimaki *et al.*, Phys. Rev. B **57**, 3920 (1998).
- [15] M. O'Keefe and G. V. Gibbs, J. Chem. Phys. **81**, 876 (1984).
- [16] T. Uchino and T. Yoko, Science **273**, 480 (1996); T. Uchino, Y. Tokuda, and T. Yoko, Phys. Rev. B **58**, 5322 (1998); T. Uchino and T. Yoko, J. Chem. Phys. **108**, 8130 (1998).
- [17] G. Pacchioni and G. Ieranó, Phys. Rev. Lett. **79**, 753 (1997).
- [18] L. A. Curtiss *et al.*, J. Chem. Phys. **103**, 6104 (1995), and references therein.
- [19] M. J. Frisch *et al.*, Gaussian 94, Revision D3, (Gaussian Inc., Pittsburgh, 1995).
- [20] M. E. Casida, C. Jamorski, K. C. Casida, and D. R. Salahub, J. Chem. Phys. **108**, 4439 (1998).
- [21] A. D. Becke, J. Chem. Phys. **98**, 5648 (1993); P. J. Stephens, F. J. Devlin, M. J. Frisch, and C. F. Chabalowski, J. Phys. Chem. **98**, 11 623 (1994).
- [22] T. E. Tsai, D. L. Griscom, and E. J. Friebele, Diffus. Defect Data, Pt. B **53-54**, 469 (1987).
- [23] D. L. Griscom and E. J. Friebele, Phys. Rev. B **34**, 7524 (1986).
- [24] R. Tohmon *et al.*, Phys. Rev. B **41**, 7258 (1990).
- [25] L. Zhang and R. G. Leisure, J. Appl. Phys. **80**, 3744 (1996).